

Incorporation of Boron, Aluminum, and Gallium Derivatives into [Ti(η^5 -C₅Me₅)(μ -O)]₃(μ_3 -CR)] (R = H, Me)

Alberto Hernán-Gómez, Avelino Martín, Miguel Mena, and Cristina Santamaría*

Departamento de Química Inorgánica, Universidad de Alcalá, 28871 Alcalá de Henares, Madrid, Spain

Received May 7, 2010

The synthesis and characterization of a family of alkyl and halide adducts of group 13 elements (B, Al, Ga), containing the μ_3 -alkylidyne oxo derivative ligands [Ti(η^5 -C₅Me₅)(μ -O)]₃(μ_3 -CR)] [R = H (**1**), Me (**2**)], are presented. The compounds are synthesized by Lewis acid–base reactions involving equimolecular amounts of **1** or **2** and alkyl [AIR'₃] (R' = Me, Et, Ph) or halide derivatives [MX₃] (M = B, X = Br; M = Al, X = Cl, Br, I; M = Ga, X = Cl, Br). The novel species [E₃M](μ_3 -O)(μ -O)₂{Ti(η^5 -C₅Me₅)]₃(μ_3 -CR)] (**3**–**8** and **11**–**21**; R = H, Me; M = B, Al, Ga; E = alkyl, halide) exhibit coordination of **1** or **2** through one of the three oxygen atoms of the Ti₃O₃ ring to the metal center. In the case of the reaction of **2** with 2 equiv of [AlMe₃], the complex [MeAl](μ_3 -O)₃{Ti(η^5 -C₅Me₅)]₃(μ_3 -CCH²⁻) (**9**) containing the naked carbanion μ_3 -CCH²⁻ was isolated with methane elimination. On the other hand, the derivative [TiBr(η^5 -C₅Me₅)](μ_3 -O)(μ -O)₂{Ti(η^5 -C₅Me₅)]₃(μ_3 -CMe)] (**11**) undergoes cleavage of the trinuclear structure to give [TiBr(η^5 -C₅Me₅)](μ -O){Ti(η^5 -C₅Me₅)](MeCBO₂){TiBr₂(η^5 -C₅Me₅)] (**22**). The crystalline structures of some of these products are also included in this paper.

Introduction

The design of macromolecular ancillary ligands has played an important role in the development of coordination chemistry. Oxygen-, nitrogen-, and phosphorus-donor macrocyclic ligands have attracted a good part of the attention.¹ The majority of synthetic efforts have been directed in order to maximize the affinity, electronic and steric, between the ancillary ligand and the metallic moiety. On some occasions, distortion of the capping ligand has been necessary to appropriately accommodate the metal fragment.

If we focus our attention on oxygen-donor macrocyclic ligands, crown ethers, calixarenes, and cryptands, undoubtedly crown ethers have contributed significantly to the development of coordination chemistry, especially group 1 and 2 metals.^{1–3} The substantial flexibility of crown ethers allows them to adapt to a variety of coordination environments and confers solubility in different media. These ligands

have important applications in the selective separation of cations and as models in molecular recognition processes.

However, although the cyclic polyethers show a great affinity for alkali metals, the use of crown ethers has been extended to other metals and inorganic compounds. In this sense, when we focus our attention on the group 13 elements, the most important and extensive chemistry bearing oxygen polydentate ligands is by far about aluminum⁴ because of the considerable Al–O bond strength. Furthermore, the chemistry of organoaluminum species and crown ethers has often been marked by distortion of the macrocyclic ligand. Thus, while alkali metal ions are placed inside the cavity of the macrocycle, alkyl derivatives of aluminum form neutral Lewis acid–base complexes along the periphery of the macrocycle. The corresponding chemistry with boron and gallium has not been developed to a comparable extent.^{1a}

The preorganized disposition of the oxo complexes [Ti(η^5 -C₅Me₅)(μ -O)]₃(μ_3 -CR)] [R = H (**1**), Me (**2**)],⁵ along with their ability to act as tridentate ligands through the oxygen atoms, gives these systems characteristics very similar to those of the metallacrown molecules described by Pecoraro et al.⁶ A few years ago, as a result of the treatment of the μ_3 -alkylidyne complexes **1** and **2** with the labile

*To whom correspondence should be addressed. E-mail: cristina.santamaria@uah.es. Fax: (+34) 91-8854683.

(1) (a) McCleverty, J. A.; Meyer, T. J.; Parkin, G. F. R. *Comprehensive Coordination Chemistry II*; Elsevier Pergamon: Oxford, U.K., 2004; Vol. 3. Wilkinson, G.; Gillard, R. D.; McCleverty, J. A. *Comprehensive Coordination Chemistry I*; Pergamon Press: Oxford, U.K., 1987; Vol. 3. (b) Ribas, J. *Química de la Coordinación*; Ediciones Omega: Barcelona, Spain, 2000. (c) Lindoy, L. F. *The Chemistry of Macrocyclic Ligand Complexes*; Cambridge University Press, Cambridge, U.K., 1989.

(2) (a) Pedersen, C. J. *J. Am. Chem. Soc.* **1967**, *89*, 2495–2496, 7017–7036. (b) Pedersen, C. J.; Friendsdorf, H. K. *Angew. Chem., Int. Ed. Engl.* **1972**, *11*, 16–25. (c) Pedersen, C. J. *Angew. Chem., Int. Ed. Engl.* **1988**, *27*, 1021–1027.

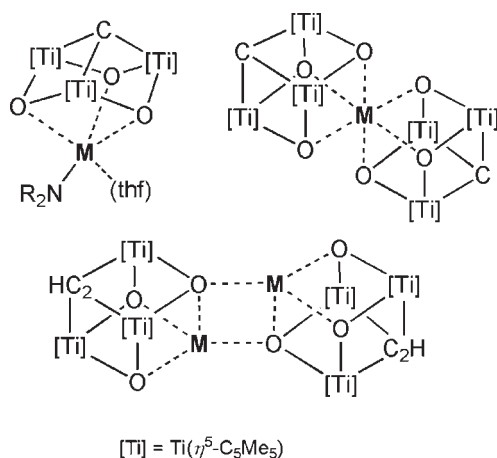
(3) Constable, E. C. *Coordination Chemistry of Macrocyclic Compounds*; Oxford University Press: New York, 1999.

(4) Holloway, C. E.; Melnik, M. *Main Group Met. Chem.* **1996**, *19*, 619–698.

(5) (a) Andrés, R.; Galakhov, M.; Martín, A.; Mena, M.; Santamaría, C. *Organometallics* **1994**, *13*, 2159–2163. (b) Andrés, R.; Galakhov, M.; Martín, A.; Mena, M.; Santamaría, C. *J. Chem. Soc., Chem. Commun.* **1995**, 551–552. (c) Andrés, R. Doctoral Thesis, Universidad de Alcalá, Alcalá de Henares, Madrid, 1995.

(6) Pecoraro, V. L.; Stemmler, A. J.; Gibney, B. R.; Bodwin, J. J.; Wang, H.; Kampf, J. W.; Barwinski, A. *Prog. Inorg. Chem.* **1997**, *45*, 83–177.

Scheme 1. Group 1 and 2 Cube-Type Derivatives



complex [Mo(CO)₃(1,3,5-Me₃C₆H₃)], we reported the formation and structure of the heterometallobutanes $\{[(\text{CO})_3\text{Mo}\{\mu_3\text{-O}\}_3\{\text{Ti}_3(\eta^5\text{-C}_5\text{Me}_5)_3(\mu_3\text{-CR})\}]\}$ (R = H, Me),⁷ in which the molybdenum tricarbonyl moiety is linked to the μ_3 -alkylidyne species through three bridging oxygen atoms. This reaction provided the starting point of an unprecedented chemistry based on the use of these titanium μ_3 -alkylidyne precursors as macrocyclic tripodal O₃ ligands.⁸ Recently, we decided to investigate the incorporation of group 1 and 2 derivatives into the vacant vertex of the incomplete cube structure of derivatives **1** and **2** (Scheme 1). In these reactions, the products exhibit a cube-type unit, where the metal cation is filling the last vertex to build new cage structures (heterometallobutane and corner- or edge-shared heterometallobutane species).⁹

The present work shows coordination of the oxo ligands **1** and **2** toward different boron, aluminum, and gallium derivatives. The coordination mode observed for the group 13 derivatives locates on the oxygen atoms of the organometallic oxides instead of on the alkylidyne moiety, as reported by Mindiola and co-workers for the complex $[(\text{PNP})\text{Ti}\equiv\text{C}^t\text{Bu}]$.¹⁰

Experimental Section

General Procedures. All manipulations of the described compounds were carried out under exclusion of air and moisture using Schlenk-line or glovebox techniques. Solvents were carefully dried from the appropriate drying agents and distilled prior to use. $\{[\text{Ti}(\eta^5\text{-C}_5\text{Me}_5)(\mu\text{-O})\}_3(\mu_3\text{-CR})\}$ [R = H (**1**), Me (**2**)] were synthesized according to the published procedures.⁵ $[\text{AlR}'_3]$ (R' = Me, Et), BBr_3 , AlI_3 , and GaBr_3 were purchased from Aldrich and AlBr_3 and GaBr_3 from Alfa-Aesar and used as received. AlCl_3 and GaCl_3 were purchased from Aldrich and sublimed before use. $[\text{AlPh}_3]$ was prepared according to

(7) Abarca, A.; Galakhov, M.; Gómez-Sal, P.; Martín, A.; Mena, M.; Poblet, J. M.; Santamaría, C.; Sarasa, J. P. *Angew. Chem.* **2000**, *112*, 544–547. *Angew. Chem., Int. Ed.* **2000**, *39*, 534–537.

(8) Gracia, J.; Martín, A.; Mena, M.; Morales-Varela, M. C.; Poblet, J.-M.; Santamaría, C. *Angew. Chem.* **2003**, *115*, 957–960. *Angew. Chem., Int. Ed.* **2003**, *42*, 927–930.

(9) (a) Martín, A.; Mena, M.; Morales-Varela, M. C.; Santamaría, C. *Eur. J. Inorg. Chem.* **2004**, 1914–1921. (b) González-del Moral, O.; Martín, A.; Mena, M.; Morales-Varela, M. C.; Santamaría, C. *Chem. Commun.* **2005**, 3682–3684. (c) Martín, A.; Mena, M.; Morales-Varela, M. C.; Santamaría, C. *Eur. J. Inorg. Chem.* **2006**, 2137–2145.

(10) Bailey, B. C.; Fout, A. R.; Fan, H.; Tomaszewski, J.; Huffman, J. C.; Mindiola, D. J. *Angew. Chem., Int. Ed.* **2007**, *46*, 8246–8249.

reported methods.¹¹ Elemental analysis (C, H, and N) was performed with a Leco CHNS-932 and/or a Perkin-Elmer 2400 Series II C, H, N, S/O. IR spectra were obtained in KBr pellets by using a Perkin-Elmer SPECTRUM 2000 Fourier transform IR spectrophotometer. NMR spectra were recorded on Varian NMR System spectrometers: Unity-300, Mercury-VX, or Unity-500 Plus. Trace amounts of protonated solvents or carbon of the solvent were used as references, and chemical shifts are reported relative to tetramethylsilane (TMS). Mass spectrometry (MS) spectra were measured with a Hewlett-Packard 5988A or a Thermo Scientific ITQ 900 spectrometer.

General Procedure for the Synthesis of $\{[\text{R}'_3\text{Al}](\mu_3\text{-O})(\mu\text{-O})_2\text{Ti}(\eta^5\text{-C}_5\text{Me}_5)_3(\mu_3\text{-CR})\}$ [R = H, R' = Et (4**), Ph (**5**); R = Me, R' = Me (**6**), Et (**7**), Ph (**8**)].** A hexane solution of the stoichiometric amount of $[\text{AlR}'_3]$ (R' = Me, Et, Ph) (5 mL) was added slowly to a solution of compound **1** or **2** in hexane (10 mL), and the mixture was left at room temperature with stirring. After 1 h, a microcrystalline solid was observed at the bottom of the Schlenk flask. The solid was separated by filtration and dried under a flux of argon.

$\{[\text{Et}_3\text{Al}](\mu_3\text{-O})(\mu\text{-O})_2\text{Ti}(\eta^5\text{-C}_5\text{Me}_5)_3(\mu_3\text{-CH})\}$ (**4**). $[\text{AlEt}_3]$ (0.57 g of a 1 M hexane solution, $\rho = 0.692 \text{ g}\cdot\text{mL}^{-1}$, 0.82 mmol) and **1** (0.50 g, 0.82 mmol) yielded **4** as an orange crystalline solid (0.41 g, 69%). IR (KBr, cm^{-1}): ν 2914 (vs), 2849 (vs), 1431 (m), 1377 (s), 1180 (w), 1023 (w), 984 (w), 946 (w), 790 (m), 688 (vs), 638 (vs), 486 (w), 446 (w), 435 (w), 418 (w), 393(s). ¹H NMR (300 MHz, $[\text{D}_6]$ benzene, 20 °C, TMS): δ 0.27 (q, ³J_{H-H} = 7.8 Hz, 6H, AlCH_2Me), 1.73 (t, ³J_{H-H} = 7.8 Hz, 9H, AlCH_2Me), 1.83 (s, 15H, C_5Me_5), 1.91 (s, 30H, C_5Me_5), 13.15 (s, 1H, $\mu_3\text{-CH}$). ¹³C NMR (75 MHz, $[\text{D}_6]$ benzene, 20 °C, TMS): δ 5.3 (t br, $J_{\text{C-H}} = 109.3 \text{ Hz}$, AlCH_2Me), 11.5 (qt, $J_{\text{C-H}} = 122.5 \text{ Hz}$, ²J_{C-H} = 5.7 Hz, AlCH_2Me), 11.9, 12.5 (q, $J_{\text{C-H}} = 125.9 \text{ Hz}$, C_5Me_5), 121.8, 123.3 (m, C_5Me_5), 401.2 (d, $J_{\text{C-H}} = 140.8 \text{ Hz}$, $\mu_3\text{-CH}$). EI-MS: m/z 610 (47%) $[\text{M} - \text{AlEt}_3]^+$. Elem. anal. calcd. (%) for $\text{C}_{37}\text{H}_{61}\text{AlO}_3\text{Ti}_3$ (724.48): C, 61.34; H, 8.49. Found: C, 62.16; H, 8.22.

$\{[\text{Ph}_3\text{Al}](\mu_3\text{-O})(\mu\text{-O})_2\text{Ti}(\eta^5\text{-C}_5\text{Me}_5)_3(\mu_3\text{-CH})\}$ (**5**). $[\text{AlPh}_3]$ (0.13 g, 0.49 mmol) and **1** (0.30 g, 0.49 mmol) yielded **5** as an orange crystalline solid (0.28 g, 65%). IR (KBr, cm^{-1}): ν 3050 (m), 2972 (m), 2911 (m), 2857 (m), 1577 (w), 1560 (w), 1479 (w), 1432 (m), 1418 (m), 1377 (m), 1246 (w), 1193 (w), 1077 (s), 1023 (w), 786 (w), 731 (m), 706 (s), 687 (vs), 657 (s), 625 (s), 608 (vs), 474 (s), 435 (s), 383 (m). ¹H NMR (300 MHz, $[\text{D}_6]$ benzene, 20 °C, TMS): δ 1.66 (s, 30H, C_5Me_5), 1.93 (s, 15H, C_5Me_5), 7.31 (3H, *p*- AlPh_3), 7.39 (6H, *m*- AlPh_3), 8.41 (6H, *o*- AlPh_3), 13.30 (s, 1H, $\mu_3\text{-CH}$). ¹³C NMR (125 MHz, $[\text{D}_6]$ benzene, 20 °C, TMS): δ 12.1, 12.3 (q, $J_{\text{C-H}} = 126.5 \text{ Hz}$, C_5Me_5), 122.2, 124.4 (m, C_5Me_5), 126.7, 127.1, 127.8, 140.9 (m, AlPh_3), 404.7 (d, $J_{\text{C-H}} = 140.9 \text{ Hz}$, $\mu_3\text{-CH}$). EI-MS: m/z 610 (2%) $[\text{M} - \text{AlPh}_3]^+$. Elem. anal. calcd. (%) for $\text{C}_{49}\text{H}_{61}\text{AlO}_3\text{Ti}_3$ (868.59): C, 67.75; H, 7.08. Found: C, 67.82; H, 7.04.

$\{[\text{Me}_3\text{Al}](\mu_3\text{-O})(\mu\text{-O})_2\text{Ti}(\eta^5\text{-C}_5\text{Me}_5)_3(\mu_3\text{-CMe})\}$ (**6**). Following the procedure described above, $[\text{AlMe}_3]$ (0.32 g of a 2 M toluene solution, $\rho = 0.810 \text{ g}\cdot\text{mL}^{-1}$, 0.80 mmol) and **2** (0.50 g, 0.80 mmol) yielded complex **6** as a brown solid (0.39 g, 70%). IR (KBr, cm^{-1}): ν 2911 (vs), 1490 (w), 1433 (m), 1376 (m), 1173 (m), 1024 (m), 792 (m), 667 (vs), 625 (vs), 427 (s), 385(s). ¹H NMR (300 MHz, $[\text{D}_6]$ benzene, 20 °C, TMS): δ -0.18 (s, 9H, AlMe), 1.90 (s, 45H, C_5Me_5), 2.77 (s, 3H, $\mu_3\text{-CMe}$). ¹³C NMR (75 MHz, $[\text{D}_6]$ benzene, 20 °C, TMS): δ -1.7 (tm, $J_{\text{C-H}} = 108.7 \text{ Hz}$, AlMe), 11.7 (qm, $J_{\text{C-H}} = 121.3 \text{ Hz}$, C_5Me_5), 42.1 (qm, $J_{\text{C-H}} = 124.7 \text{ Hz}$, $\mu_3\text{-CMe}$), 122.8 (m, C_5Me_5), 418.1 (s, $\mu_3\text{-CMe}$). EI-MS: m/z 666 (4%) $[\text{M} - \text{Me}_2]^+$, 624 (25%) $[\text{M} - \text{AlMe}_3]^+$. Elem. anal. calcd. (%) for $\text{C}_{35}\text{H}_{57}\text{AlO}_3\text{Ti}_3$ (696.43): C, 60.36; H, 8.25. Found: C, 60.58; H, 7.61.

$\{[\text{Et}_3\text{Al}](\mu_3\text{-O})(\mu\text{-O})_2\text{Ti}(\eta^5\text{-C}_5\text{Me}_5)_3(\mu_3\text{-CMe})\}$ (**7**). $[\text{AlEt}_3]$ (0.55 g of a 1 M hexane solution, $\rho = 0.692 \text{ g}\cdot\text{mL}^{-1}$, 0.80 mmol)

(11) Mole, T. *Aust. J. Chem.* **1963**, *16*, 794–800.

and **2** (0.50 g, 0.80 mmol) yielded **7** as brown crystals (0.40 g, 68%). IR (KBr, cm^{-1}): $\bar{\nu}$ 2912 (vs), 2849 (vs), 1490 (w), 1430 (m), 1376 (s), 1229 (w), 1180 (w), 1164 (w), 1066 (w), 1023 (w), 986 (w), 947 (w), 790 (w), 668 (vs), 630 (vs), 604 (s), 589 (s), 485 (w), 465 (w), 424 (s), 384 (m). ^1H NMR (300 MHz, $[\text{D}_6]\text{benzene}$, 20 °C, TMS): δ 0.27 (q, $^3J_{\text{H-H}} = 8.1$ Hz, 6H, AlCH_2Me), 1.71 (t, $^3J_{\text{H-H}} = 8.1$ Hz, 9H, AlCH_2Me), 1.90 (s, 45H, C_5Me_5), 2.76 (s, 3H, $\mu_3\text{-CMe}$). $^{13}\text{C}\{^1\text{H}\}$ NMR (75 MHz, $[\text{D}_6]\text{benzene}$, 20 °C, TMS): δ 5.6 (AlCH_2Me), AlCH_2Me (signal not detected), 11.7 (C_5Me_5), 41.7 ($\mu_3\text{-CMe}$), 122.7 (C_5Me_5), 418.4 ($\mu_3\text{-CMe}$). EI-MS: m/z 680 (11%) $[\text{M} - 2\text{Et}]^+$; 624 (14%) $[\text{M} - \text{AlEt}_3]^+$. Elem. anal. calcd. (%) for $\text{C}_{38}\text{H}_{63}\text{AlO}_3\text{Ti}_3$ (738.50): C, 61.80; H, 8.60. Found: C, 62.07; H, 8.36.

$[\{\text{Ph}_3\text{Al}\}(\mu_3\text{-O})(\mu\text{-O})_2\{\text{Ti}(\eta^5\text{-C}_5\text{Me}_5)_3(\mu_3\text{-CMe})\}]$ (**8**). $[\text{AlPh}_3]$ (0.13 g, 0.48 mmol) and **2** (0.30 g, 0.48 mmol) yielded **8** as brown crystals (0.31 g, 72%). IR (KBr, cm^{-1}): $\bar{\nu}$ 3051 (m), 2908 (s), 2857 (m), 1576 (w), 1559 (w), 1480 (w), 1419 (m), 1377 (m), 1246 (w), 1193 (w), 1163 (w), 1077 (m), 1022 (w), 791 (w), 731 (w), 704 (s), 670 (vs), 605 (vs), 472 (s), 436 (s), 374 (m). ^1H NMR (300 MHz, $[\text{D}_6]\text{benzene}$, 20 °C, TMS): δ 1.66 (s, 30H, C_5Me_5), 1.92 (s, 15H, C_5Me_5), 2.78 (s, 3H, $\mu_3\text{-CMe}$), 7.31 (3H, *p*- AlPh_3), 7.38 (6H, *m*- AlPh_3), 8.37 (6H, *o*- AlPh_3). ^{13}C NMR (75 MHz, $[\text{D}_6]\text{benzene}$, 20 °C, TMS): δ 11.4, 12.2 (q, $J_{\text{C-H}} = 125.9$ Hz, C_5Me_5), 42.2 (q, $J_{\text{C-H}} = 127.0$ Hz, $\mu_3\text{-CMe}$), 122.5, 124.3 (m, C_5Me_5), 126.4, 126.8, 128.6, 141.1 (m, AlPh_3), 420.0 (s, $\mu_3\text{-CMe}$). EI-MS: m/z 624 (24%) $[\text{M} - \text{AlPh}_3]^+$. Elem. anal. calcd. (%) for $\text{C}_{50}\text{H}_{63}\text{AlO}_3\text{Ti}_3$ (882.62): C, 68.03; H, 7.19. Found: C, 67.40; H, 7.92.

$[\{\text{MeAl}\}(\mu_3\text{-O})_3\{\text{Ti}(\eta^5\text{-C}_5\text{Me}_5)_3(\mu_3\text{-CCH}_2^-)\}]$ (**9**). $[\text{AlMe}_3]$ (0.17 g of a 1 M hexane solution, $\rho = 0.810$ g·mL $^{-1}$, 0.43 mmol) and **6** (0.30 g, 0.43 mmol) yielded **9** as a black solid (0.14 g, 48%). IR (KBr, cm^{-1}): $\bar{\nu}$ 2908 (vs), 1687 (w), 1492 (m), 1432 (s), 1375 (s), 1281 (w), 1180 (s), 1067 (w), 1024 (m), 908 (m), 741 (vs), 692 (vs), 625 (s), 582 (s), 534 (s), 461 (m), 434 (m). ^1H NMR (300 MHz, $[\text{D}_6]\text{benzene}$, 20 °C, TMS): δ -0.50 (s, 3H, AlMe), 1.81 (s, 30H, C_5Me_5), 2.13 (s, 15H, C_5Me_5), 9.42 (s, 1H, $\mu_3\text{-CCH}_2^-$). $^{13}\text{C}\{^1\text{H}\}$ NMR (75 MHz, $[\text{D}_6]\text{benzene}$, 20 °C, TMS): δ -17.9 (AlMe), 11.4, 12.1 (C_5Me_5), 118.1, 120.7 (C_5Me_5), 235.5 ($\mu_3\text{-CCH}_2^-$), 329.4 ($\mu_3\text{-CCH}_2^-$). Elem. anal. calcd. (%) for $\text{C}_{33}\text{H}_{49}\text{AlO}_3\text{Ti}_3$ (664.34): C, 59.66; H, 7.43. Found: C, 59.24; H, 7.61.

Preparation of $[\{\text{Br}_3\text{B}\}(\mu_3\text{-O})(\mu\text{-O})_2\{\text{Ti}(\eta^5\text{-C}_5\text{Me}_5)_3(\mu_3\text{-CMe})\}]$ (11**).** BBr_3 (0.69 g of a 1 M hexane solution, $\rho = 0.859$ g·mL $^{-1}$, 0.80 mmol) diluted in 10 mL of toluene was added over a toluene solution (30 mL) of **2** (0.50 g, 0.80 mmol). The solution was left stirring for 15 min, then concentrated under vacuum to ≈ 15 mL, and cooled to -35 °C, yielding complex **11** as a dark-red microcrystalline solid (0.23 g, 32%). IR (KBr, cm^{-1}): $\bar{\nu}$ 2906 (s), 1488 (w), 1430 (m), 1376 (s), 1101 (w), 1069 (w), 1023 (w), 943 (w), 910 (w), 877 (s), 849 (vs), 712 (s), 629 (s), 554 (w), 517 (vs), 482 (w), 445 (s), 429 (s). ^1H NMR (300 MHz, $[\text{D}_6]\text{benzene}$, 20 °C, TMS): δ 2.00 (s, 30H, C_5Me_5), 2.18 (s, 15H, C_5Me_5), 2.88 (s, 3H, $\mu_3\text{-CMe}$). ^{13}C NMR (75 MHz, $[\text{D}_6]\text{benzene}$, 20 °C, TMS): δ 12.3, 14.1 (q, $J_{\text{C-H}} = 125.9$ Hz, C_5Me_5), 44.5 (q, $J_{\text{C-H}} = 127.0$ Hz, $\mu_3\text{-CMe}$), 123.9, 134.7 (m, C_5Me_5), 499.4 (s, $\mu_3\text{-CMe}$). Elem. anal. calcd. (%) for $\text{C}_{32}\text{H}_{48}\text{BBr}_3\text{O}_3\text{Ti}_3$ (874.86): C, 43.93; H, 5.53. Found: C, 43.97; H, 5.42.

General Procedure for the Synthesis of $[\{\text{X}_3\text{M}\}(\mu_3\text{-O})(\mu\text{-O})_2\{\text{Ti}(\eta^5\text{-C}_5\text{Me}_5)_3(\mu_3\text{-CR})\}]$ [M** = Al; **X** = Cl, **R** = H (**12**), **Me** (**13**); **X** = Br, **R** = H (**14**), **Me** (**15**); **X** = I, **R** = H (**16**), **Me** (**17**); **M** = Ga; **X** = Cl, **R** = H (**18**), **Me** (**19**); **X** = Br, **R** = H (**20**), **Me** (**21**)].** A toluene suspension (10 mL) of the corresponding equimolecular amount of MX_3 was added to a solution of **1** or **2** in toluene (20 mL). The mixture was left at room temperature with stirring for 15 min. Then the solution was concentrated to 15 mL, getting precipitates of complexes **13**, **15**, and **17–21**, while **12**, **14**, and **16** precipitated after the solution was cooled to -35 °C. Solids were separated by filtration and dried under a flux of argon.

Preparation of $[\{\text{Cl}_3\text{Al}\}(\mu_3\text{-O})(\mu\text{-O})_2\{\text{Ti}(\eta^5\text{-C}_5\text{Me}_5)_3(\mu_3\text{-CH})\}]$ (12**).** Following the procedure described above, AlCl_3

(0.065 g, 0.49 mmol) and **1** (0.30 g, 0.49 mmol) yielded complex **12** as a red microcrystalline solid (0.16 g, 44%). IR (KBr, cm^{-1}): $\bar{\nu}$ 2912 (vs), 1700 (w), 1490 (w), 1433 (m), 1378 (s), 1248 (w), 1166 (w), 1067 (w), 1025 (m), 916 (w), 878 (w), 791 (s), 742 (s), 687 (vs), 603 (s), 503 (m), 396 (m). ^1H NMR (300 MHz, $[\text{D}_6]\text{benzene}$, 20 °C, TMS): δ 1.74 (s, 15H, C_5Me_5), 1.97 (s, 30H, C_5Me_5), 13.43 (s, 1H, $\mu_3\text{-CH}$). ^{13}C NMR (75 MHz, $[\text{D}_6]\text{benzene}$, 20 °C, TMS): δ 11.9, 12.8 (q, $J_{\text{C-H}} = 126.5$ Hz, C_5Me_5), 122.8, 125.7 (m, C_5Me_5), 407.1 (d, $J_{\text{C-H}} = 140.8$ Hz, $\mu_3\text{-CH}$). Elem. anal. calcd. (%) for $\text{C}_{31}\text{H}_{46}\text{AlCl}_3\text{O}_3\text{Ti}_3$ (743.65): C, 50.06; H, 6.23. Found: C, 50.86; H, 5.76.

Preparation of $[\{\text{Cl}_3\text{Al}\}(\mu_3\text{-O})(\mu\text{-O})_2\{\text{Ti}(\eta^5\text{-C}_5\text{Me}_5)_3(\mu_3\text{-CMe})\}]$ (13**).** Following the procedure described above, AlCl_3 (0.064 g, 0.48 mmol) and **2** (0.30 g, 0.48 mmol) yielded complex **13** as a brown microcrystalline solid (0.19 g, 52%). IR (KBr, cm^{-1}): $\bar{\nu}$ 2911 (s), 1488 (w), 1427 (m), 1377 (s), 1162 (w), 1065 (w), 1023 (w), 983 (w), 887 (w), 764 (w), 716 (vs), 666 (vs), 627 (vs), 601 (vs), 504 (vs), 475 (w), 425 (m), 380 (m). ^1H NMR (300 MHz, $[\text{D}_1]\text{chloroform}$, 20 °C, TMS): δ 1.95 (s, 15H, C_5Me_5), 2.06 (s, 30H, C_5Me_5), 3.04 (s, 3H, $\mu_3\text{-CMe}$). ^{13}C NMR (75 MHz, $[\text{D}_1]\text{chloroform}$, 20 °C, TMS): δ 11.3, 12.5 (q, $J_{\text{C-H}} = 126.4$ Hz, C_5Me_5), 43.4 (q, $J_{\text{C-H}} = 125.8$ Hz, $\mu_3\text{-CMe}$), 123.1, 125.8 (m, C_5Me_5), 425.9 (s, $\mu_3\text{-CMe}$). Elem. anal. calcd. (%) for $\text{C}_{32}\text{H}_{48}\text{AlCl}_3\text{O}_3\text{Ti}_3$ (757.67): C, 50.72; H, 6.38. Found: C, 50.43; H, 6.06.

Preparation of $[\{\text{Br}_3\text{Al}\}(\mu_3\text{-O})(\mu\text{-O})_2\{\text{Ti}(\eta^5\text{-C}_5\text{Me}_5)_3(\mu_3\text{-CH})\}]$ (14**).** Following the procedure described above, AlBr_3 (0.131 g, 0.49 mmol) and **1** (0.30 g, 0.49 mmol) yielded complex **14** as a dark-red microcrystalline solid (0.18 g, 41%). IR (KBr, cm^{-1}): $\bar{\nu}$ 2910 (s), 1488 (w), 1431 (m), 1377 (s), 1164 (w), 1067 (w), 1023 (w), 887 (br w), 785 (m), 731 (s), 686 (vs), 600 (vs), 491 (w), 459 (w), 425 (s), 387 (m). ^1H NMR (300 MHz, $[\text{D}_6]\text{benzene}$, 20 °C, TMS): δ 1.75 (s, 15H, C_5Me_5), 1.99 (s, 30H, C_5Me_5), 13.48 (s, 1H, $\mu_3\text{-CH}$). ^{13}C NMR (75 MHz, $[\text{D}_6]\text{benzene}$, 20 °C, TMS): δ 12.0, 13.2 (q, $J_{\text{C-H}} = 126.4$ Hz, C_5Me_5), 122.9, 125.8 (m, C_5Me_5), 408.7 (d, $J_{\text{C-H}} = 141.3$ Hz, $\mu_3\text{-CH}$). EI-MS: m/z 717 (2%) $[\text{M} - 2\text{Br}]^+$, 637 (2%) $[\text{M} - 3\text{Br}]^+$, 610 (6%) $[\text{M} - \text{AlBr}_3]^+$. Elem. anal. calcd. (%) for $\text{C}_{31}\text{H}_{46}\text{AlBr}_3\text{O}_3\text{Ti}_3$ (877.00): C, 42.45; H, 5.29. Found: C, 42.85; H, 5.15.

Preparation of $[\{\text{Br}_3\text{Al}\}(\mu_3\text{-O})(\mu\text{-O})_2\{\text{Ti}(\eta^5\text{-C}_5\text{Me}_5)_3(\mu_3\text{-CMe})\}]$ (15**).** Following the procedure described above, AlBr_3 (0.128 g, 0.48 mmol) and **2** (0.30 g, 0.48 mmol) yielded complex **15** as a brown microcrystalline solid (0.22 g, 52%). IR (KBr, cm^{-1}): $\bar{\nu}$ 2910 (s), 1489 (w), 1427 (m), 1377 (s), 1163 (w), 1066 (w), 1023 (w), 901 (br w), 785 (m), 757 (m), 711 (s), 665 (vs), 625 (s), 599 (vs), 463 (w), 426 (s), 377 (w). ^1H NMR (500 MHz, $[\text{D}_1]\text{chloroform}$, 20 °C, TMS): δ 1.95 (s, 15H, C_5Me_5), 2.09 (s, 30H, C_5Me_5), 3.03 (s, 3H, $\mu_3\text{-CMe}$). ^{13}C NMR (125 MHz, $[\text{D}_1]\text{chloroform}$, 20 °C, TMS): δ 11.4, 12.8 (q, $J_{\text{C-H}} = 126.1$ Hz, C_5Me_5), 42.9 (q, $J_{\text{C-H}} = 126.8$ Hz, $\mu_3\text{-CMe}$), 123.1, 125.9 (m, C_5Me_5), 427.1 (bs, $\mu_3\text{-CMe}$). EI-MS: m/z 891 (9%) $[\text{M}]^+$, 651 (6%) $[\text{M} - 3\text{Br}]^+$, 624 (29%) $[\text{M} - \text{AlBr}_3]^+$. Elem. anal. calcd. (%) for $\text{C}_{32}\text{H}_{48}\text{AlBr}_3\text{O}_3\text{Ti}_3$ (891.02): C, 43.13; H, 5.43. Found: C, 43.15; H, 5.02.

Preparation of $[\{\text{I}_3\text{Al}\}(\mu_3\text{-O})(\mu\text{-O})_2\{\text{Ti}(\eta^5\text{-C}_5\text{Me}_5)_3(\mu_3\text{-CH})\}]$ (16**).** Following the procedure described above, AlI_3 (0.200 g, 0.49 mmol) and **1** (0.30 g, 0.49 mmol) yielded compound **16** as a red microcrystalline solid (0.30 g, 59%). IR (KBr, cm^{-1}): $\bar{\nu}$ 2908 (s), 1485 (w), 1430 (m), 1377 (s), 1163 (w), 1067 (w), 1022 (w), 900 (br w), 793 (s), 724 (s), 684 (vs), 599 (vs), 501 (w), 435 (w), 391 (w). ^1H NMR (300 MHz, $[\text{D}_6]\text{benzene}$, 20 °C, TMS): δ 1.75 (s, 15H, C_5Me_5), 2.02 (s, 30H, C_5Me_5), 13.52 (s, 1H, $\mu_3\text{-CH}$). ^{13}C NMR (75 MHz, $[\text{D}_6]\text{benzene}$, 20 °C, TMS): δ 12.1, 13.8 (q, $J_{\text{C-H}} = 126.4$ Hz, C_5Me_5), 123.2, 126.0 (m, C_5Me_5), 410.8 (d, $J_{\text{C-H}} = 140.8$ Hz, $\mu_3\text{-CH}$). EI-MS: m/z 763 (11%) $[\text{M} - \text{H} - 2\text{I}]^+$, 624 (12%) $[\text{M} - \text{CH} - 3\text{I}]^+$. Elem. anal. calcd. (%) for $\text{C}_{31}\text{H}_{46}\text{AlI}_3\text{O}_3\text{Ti}_3$ (1018.00): C, 36.57; H, 4.55. Found: C, 36.44; H, 4.88.

Preparation of $[\{\text{I}_3\text{Al}\}(\mu_3\text{-O})(\mu\text{-O})_2\{\text{Ti}(\eta^5\text{-C}_5\text{Me}_5)_3(\mu_3\text{-CMe})\}]$ (17**).** Following the procedure described above, AlI_3 (0.196 g, 0.48 mmol) and **2** (0.30 g, 0.48 mmol) yielded complex

17 as a brown microcrystalline solid (0.16 g, 32%). IR (KBr, cm^{-1}): $\bar{\nu}$ 2909 (s), 1489 (w), 1428 (m), 1377 (s), 1162 (w), 1067 (w), 1023 (w), 897 (br w), 777 (s), 729 (m), 701 (s), 663 (vs), 622 (s), 595 (vs), 453 (w), 422 (m), 389 (m). ^1H NMR (300 MHz, $[\text{D}_1]\text{chloroform}$, 20 °C, TMS): δ 1.95 (s, 15H, C_5Me_5), 2.13 (s, 30H, C_5Me_5), 2.97 (s, 3H, $\mu_3\text{-CMe}$). $^{13}\text{C}\{^1\text{H}\}$ NMR (75 MHz, $[\text{D}_1]\text{chloroform}$, 20 °C, TMS): δ 11.4, 13.4 (C_5Me_5), 41.2 ($\mu_3\text{-CMe}$), 125.3, 126.0 (C_5Me_5), 426.3 ($\mu_3\text{-CMe}$). Elem. anal. calcd. (%) for $\text{C}_{32}\text{H}_{48}\text{Al}_3\text{O}_3\text{Ti}_3$ (1032.04): C, 37.24; H, 4.69. Found: C, 37.04; H, 4.71.

Preparation of $[\{\text{Cl}_3\text{Ga}\}(\mu_3\text{-O})(\mu\text{-O})_2\{\text{Ti}(\eta^5\text{-C}_5\text{Me}_5)\}_3(\mu_3\text{-CH})]$ (18). Following the procedure described above, GaCl_3 (0.086 g, 0.49 mmol) and **1** (0.30 g, 0.49 mmol) yielded compound **18** as a red microcrystalline solid (0.21 g, 54%). IR (KBr, cm^{-1}): $\bar{\nu}$ 2911 (s), 1489 (w), 1431 (m), 1378 (s), 1261 (w), 1164 (w), 1067 (w), 1023 (w), 842 (m), 791 (s), 749 (m), 699 (vs), 662 (vs), 626 (s), 601 (vs), 440 (m), 392 (s). ^1H NMR (300 MHz, $[\text{D}_6]\text{benzene}$, 20 °C, TMS): δ 1.75 (s, 15H, C_5Me_5), 1.97 (s, 30H, C_5Me_5), 13.37 (s, 1H, $\mu_3\text{-CH}$). ^{13}C NMR (75 MHz, $[\text{D}_6]\text{benzene}$, 20 °C, TMS): δ 11.9, 12.8 (q, $J_{\text{C-H}} = 125.9$ Hz, C_5Me_5), 122.8, 125.4 (m, C_5Me_5), 406.2 (d, $J_{\text{C-H}} = 140.8$ Hz, $\mu_3\text{-CH}$). EI-MS: m/z 610 (7%) $[\text{M} - \text{GaCl}_3]^+$. Elem. anal. calcd. (%) for $\text{C}_{31}\text{H}_{46}\text{Cl}_3\text{GaO}_3\text{Ti}_3$ (786.39): C, 47.34; H, 5.90. Found: C, 47.37; H, 5.65.

Preparation of $[\{\text{Cl}_3\text{Ga}\}(\mu_3\text{-O})(\mu\text{-O})_2\{\text{Ti}(\eta^5\text{-C}_5\text{Me}_5)\}_3(\mu_3\text{-CMe})]$ (19). Following the procedure described above, GaCl_3 (0.084 g, 0.48 mmol) and **2** (0.30 g, 0.48 mmol) yielded compound **19** as a brown microcrystalline solid (0.23 g, 59%). IR (KBr, cm^{-1}): $\bar{\nu}$ 2911 (s), 1492 (w), 1429 (s), 1378 (s), 1162 (w), 1067 (w), 1024 (w), 838 (w), 787 (s), 745 (s), 681 (vs), 657 (vs), 628 (vs), 601 (vs), 443 (w), 426 (w), 387 (s). ^1H NMR (300 MHz, $[\text{D}_1]\text{chloroform}$, 20 °C, TMS): δ 1.95 (s, 15H, C_5Me_5), 2.05 (s, 30H, C_5Me_5), 3.02 (s, 3H, $\mu_3\text{-CMe}$). ^{13}C NMR (75 MHz, $[\text{D}_1]\text{chloroform}$, 20 °C, TMS): δ 11.4, 12.4 (q, $J_{\text{C-H}} = 125.9$ Hz, C_5Me_5), 43.0 (q, $J_{\text{C-H}} = 127.0$ Hz, $\mu_3\text{-CMe}$), 123.2, 125.3 (m, C_5Me_5), 425.6 (s, $\mu_3\text{-CMe}$). Elem. anal. calcd. (%) for $\text{C}_{32}\text{H}_{48}\text{GaCl}_3\text{O}_3\text{Ti}_3$ (800.42): C, 48.01; H, 6.04. Found: C, 48.73; H, 5.99.

Preparation of $[\{\text{Br}_3\text{Ga}\}(\mu_3\text{-O})(\mu\text{-O})_2\{\text{Ti}(\eta^5\text{-C}_5\text{Me}_5)\}_3(\mu_3\text{-CH})]$ (20). Following the procedure described above, GaBr_3 (0.152 g, 0.49 mmol) and **1** (0.30 g, 0.49 mmol) yielded complex **20** as a red microcrystalline solid (0.25 g, 56%). IR (KBr, cm^{-1}): $\bar{\nu}$ 2911 (s), 1489 (w), 1431 (m), 1377 (s), 1164 (w), 1067 (w), 1023 (w), 839 (w), 785 (m), 697 (vs), 659 (vs), 626 (vs), 601 (vs), 438 (m), 393 (m). ^1H NMR (300 MHz, $[\text{D}_6]\text{benzene}$, 20 °C, TMS): δ 1.76 (s, 15H, C_5Me_5), 1.99 (s, 30H, C_5Me_5), 13.39 (s, 1H, $\mu_3\text{-CH}$). ^{13}C NMR (75 MHz, $[\text{D}_6]\text{benzene}$, 20 °C, TMS): δ 12.0, 13.1 (q, $J_{\text{C-H}} = 125.9$ Hz, C_5Me_5), 122.8, 125.4 (m, C_5Me_5), 407.6 (d, $J_{\text{C-H}} = 140.8$ Hz, $\mu_3\text{-CH}$). Elem. anal. calcd. (%) for $\text{C}_{31}\text{H}_{46}\text{Br}_3\text{GaO}_3\text{Ti}_3$ (919.74): C, 40.48; H, 5.04. Found: C, 40.43; H, 5.07.

Preparation of $[\{\text{Br}_3\text{Ga}\}(\mu_3\text{-O})(\mu\text{-O})_2\{\text{Ti}(\eta^5\text{-C}_5\text{Me}_5)\}_3(\mu_3\text{-CMe})]$ (21). Following the procedure described above, GaBr_3 (0.148 g, 0.48 mmol) and **2** (0.30 g, 0.48 mmol) yielded complex **21** as a brown microcrystalline solid (0.28 g, 62%). IR (KBr, cm^{-1}): $\bar{\nu}$ 2910 (s), 1489 (w), 1427 (m), 1377 (s), 1163 (w), 1066 (w), 1023 (w), 785 (s), 731 (m), 678 (vs), 658 (vs), 624 (vs), 600 (vs), 461 (w), 441 (w), 426 (w), 383 (m). ^1H NMR (300 MHz, $[\text{D}_1]\text{chloroform}$, 20 °C, TMS): δ 1.95 (s, 15H, C_5Me_5), 2.08 (s, 30H, C_5Me_5), 3.00 (s, 3H, $\mu_3\text{-CMe}$). ^{13}C NMR (75 MHz, $[\text{D}_1]\text{chloroform}$, 20 °C, TMS): δ 11.4, 12.7 (q, $J_{\text{C-H}} = 126.4$ Hz, C_5Me_5), 42.5 (q, $J_{\text{C-H}} = 127.0$ Hz, $\mu_3\text{-CMe}$), 123.3, 125.3 (m, C_5Me_5), 425.5 (s, $\mu_3\text{-CMe}$). Elem. anal. calcd. (%) for $\text{C}_{32}\text{H}_{48}\text{Br}_3\text{GaO}_3\text{Ti}_3$ (933.77): C, 41.16; H, 5.18. Found: C, 41.61; H, 4.95.

Preparation of $[\{\text{TiBr}(\eta^5\text{-C}_5\text{Me}_5)\}(\mu\text{-O})\{\text{Ti}(\eta^5\text{-C}_5\text{Me}_5)\}_2(\text{MeCBO}_2)\{\text{TiBr}_2(\eta^5\text{-C}_5\text{Me}_5)\}]$ (22). Compound **11** (0.26 g, 0.29 mmol) was left stirring in 20 mL of toluene for 2 days at room temperature. After that, the reaction mixture was cooled to -35 °C to afford complex **22**· $\frac{1}{2}\text{C}_7\text{H}_8$ as an orange microcrystalline solid. Yield: 0.08 g, 29%. IR (KBr, cm^{-1}): $\bar{\nu}$ 2977 (w),

2952 (w), 2910 (m), 2857 (w), 1494 (w), 1430 (m), 1378 (m), 1296 (s), 1252 (vs), 1156 (bs), 1064 (vs), 1023 (m), 729 (m), 673 (s), 585 (s), 560 (s), 542 (s), 447 (m), 430 (m). ^1H NMR (300 MHz, $[\text{D}_6]\text{benzene}$, 20 °C, TMS): δ 2.07, 2.11, 2.21 (s, 15H, C_5Me_5), 2.09 (s, 3H, MeCBO_2). ^{13}C NMR (75 MHz, $[\text{D}_6]\text{benzene}$, 20 °C, TMS): δ 11.6, 12.8, 14.1 (q, $J_{\text{C-H}} = 125.9$ Hz, C_5Me_5), 20.9 (q, $J_{\text{C-H}} = 128.2$ Hz, MeCBO_2), 124.8, 126.5, 133.6 (m, C_5Me_5), MeCBO_2 (signal not observed). EI-MS: m/z 612 (2%) $[\text{M} - \text{Ti}(\text{C}_5\text{Me}_5)\text{Br}]^+$, 585 (4%) $[\text{M} - \text{Ti}(\text{C}_5\text{Me}_5)\text{Br} - \text{CCH}_3]^+$, 343 (16%) $[\text{Ti}(\text{C}_5\text{Me}_5)\text{Br}_2]^+$. Elem. anal. calcd. (%) for $\text{C}_{32}\text{H}_{48}\text{BBr}_3\text{O}_3\text{Ti}_3 \cdot \frac{1}{2}(\text{C}_7\text{H}_8)$ (920.92): C, 46.29; H, 5.69. Found: C, 46.29; H, 5.45.

X-ray Structure Analysis of 7, 8, 10, 13, and 22. Crystals of complexes **7**, **8**, and **13** were grown from saturated hexane solutions at room temperature, and **10** was grown from a pentane solution by slow cooling of the reaction mixture and **22** from a toluene/hexane double layer. Then crystals were removed from the Schlenk flasks and covered with a layer of a viscous perfluoropolyether (Fomblin Y). A suitable crystal was selected with the aid of a microscope, attached to a glass fiber, and immediately placed in the low-temperature nitrogen stream of the diffractometer. The intensity data sets were collected at 200 K on a Bruker-Nonius Kappa CCD diffractometer equipped with an Oxford Cryostream 700 unit. Crystallographic data for all of the complexes are presented in Table 1. The structures were solved, using the *WINGX* package,¹² by direct methods (*SHELXS-97*) and refined by least squares against F^2 (*SHELXL-97*).¹³

All non-hydrogen atoms of complex **7**, **8**, and **10** were anisotropically refined. The hydrogen atoms were positioned geometrically and refined by using a riding model except those linked to C1, C2, C3, and C52 of complex **10** and those of the aromatic rings in **8**, which were located in the Fourier difference map and isotropically refined.

Complex **13** crystallized with a half-molecule of hexane and diffracted very weakly (maximum $\theta = 21.7^\circ$). It was not possible to get a chemical-sensible model for the solvent, so the SQUEEZE¹⁴ procedure was used to remove its contribution to the structure factors. All non-hydrogen atoms of **13** were anisotropically refined. The hydrogen atoms were positioned geometrically and refined by using a riding model.

Crystals of complex **22** also diffracted very weakly, and the data collection could only be performed up to $\theta = 25^\circ$. From the difference Fourier map, it was clear that two molecules of toluene crystallized in each unit cell of **22**. Both molecules presented severe disorder, and it was not possible to get a chemical-sensible model, so the SQUEEZE¹⁴ procedure was applied to remove its contribution to the structure factors. All of the non-hydrogen atoms of **22** were anisotropically refined except C30, and the hydrogen atoms were positioned geometrically and refined by using a riding model.

CCDC 772512 (**7**), 772513 (**8**), 772508 (**10**), 772510 (**13**), and 772511 (**22**) contain the supplementary crystallographic data for this paper. These data can be obtained free of charge from The Cambridge Crystallographic Data Centre via www.ccdc.cam.ac.uk/data_request/cif.

Results and Discussion

Coordination of $[\{\text{Ti}(\eta^5\text{-C}_5\text{Me}_5)(\mu\text{-O})\}_3(\mu_3\text{-CR})]$ [R** = **H** (**1**), **Me** (**2**)] to Trialkyl- or Arylaluminum Derivatives AIR'_3 (**R** = **Me**, **Et**, **Ph**).** The treatment of **1** and **2** with trimethyl-, triethyl-, or triphenylaluminum in hexane at room temperature led to the precipitation of adduct derivatives $[\{\text{R}'_3\text{Al}\}(\mu_3\text{-O})(\mu\text{-O})_2\{\text{Ti}(\eta^5\text{-C}_5\text{Me}_5)\}_3(\mu_3\text{-CR})]$

(12) Farrugia, L. J. *J. Appl. Crystallogr.* **1999**, *32*, 837–838.

(13) Sheldrick, G. M. *Acta Crystallogr.* **2008**, *A64*, 112–122.

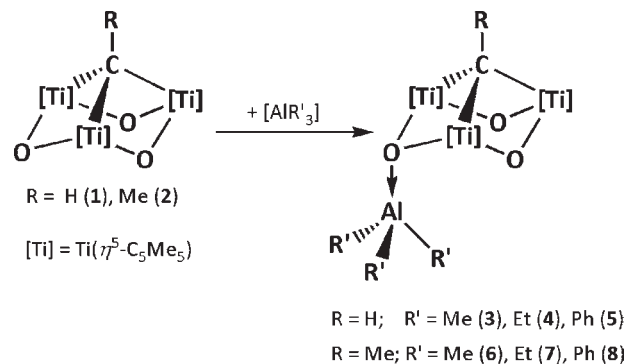
(14) SQUEEZE: Sluis, P. v. d.; Spek, A. L. *Acta Crystallogr., Sect. A* **1990**, *46*, 194–201.

Table 1. Crystal Data and Structure Refinement for 7, 8, 10, 13, and 22

| | 7 | 8 | 10 | 13 · 1/2 C ₆ H ₁₄ | 22 · C ₇ H ₈ |
|---|--|--|--|---|---|
| empirical formula | C ₃₈ H ₆₅ AlO ₃ Ti ₃ | C ₅₀ H ₆₃ AlO ₃ Ti ₃ | C ₃₉ H ₆₈ Al ₃ O ₃ Ti ₃ | C ₃₂ H ₄₈ AlCl ₃ O ₃ Ti ₃ · 1/2 C ₆ H ₁₄ | C ₃₂ H ₄₈ BBR ₃ O ₃ Ti ₃ · C ₇ H ₈ |
| formula weight | 738.56 | 882.68 | 809.57 | 800.82 | 967.08 |
| temperature [K] | 200(2) | 200(2) | 200(2) | 200(2) | 200(2) |
| wavelength (Mo Kα) [Å] | 0.71073 | 0.71073 | 0.71073 | 0.71073 | 0.71073 |
| cryst syst | monoclinic | triclinic | triclinic | monoclinic | triclinic |
| space group | P2 ₁ /n | P1 | P1 | P2 ₁ /n | P1 |
| a [Å]; α [deg] | 10.804(3) | 11.226(1); 88.08(1) | 11.557(1); 89.71(1) | 11.565(1) | 9.424(1); 80.42(1) |
| b [Å]; β [deg] | 18.837(9); 91.27(2) | 12.280(2); 82.78(1) | 11.569(2); 81.96(1) | 18.162(6); 90.90(2) | 12.203(2); 86.75(1) |
| c [Å]; γ [deg] | 19.881(13) | 18.959(2); 63.86(1) | 18.508(3); 64.72(1) | 19.207(6) | 19.523(2); 72.17(1) |
| volume [Å ³]; Z | 4045(3); 4 | 2326.9(5); 2 | 2211.5(5); 2 | 4033.8(18); 4 | 2107.5(4); 2 |
| ρ _{calc} [g · cm ⁻³] | 1.213 | 1.260 | 1.216 | 1.319 | 1.524 |
| μ [mm ⁻¹] | 0.631 | 0.560 | 0.62 | 0.831 | 3.432 |
| R(000) | 1576 | 932 | 862 | 1676 | 980 |
| cryst size [mm ³] | 0.20 × 0.13 × 0.11 | 0.36 × 0.33 × 0.27 | 0.46 × 0.23 × 0.17 | 0.19 × 0.14 × 0.12 | 0.44 × 0.36 × 0.18 |
| θ range [deg] | 3.02–27.55 | 3.14–27.50 | 3.03–27.50 | 3.03–27.69 | 3.02–25 |
| index ranges | –14 to +14, –24 to +24, 0 to 25 | –14 to +14, –15 to +15, –24 to +24 | –14 to +15, –15 to +14, –24 to +24 | –12 to +12, –18 to +18, 0 to 19 | –11 to +11, –14 to +14, –21 to +23 |
| collected reflns | 70137 | 38982 | 46695 | 47681 | 13059 |
| indep reflns | 9284 [R _{int} = 0.102] | 10573 [R _{int} = 0.093] | 10012 [R _{int} = 0.068] | 4730 [R _{int} = 0.056] | 6931 [R _{int} = 0.125] |
| GOF on F ² | 0.997 | 1.068 | 1.042 | 1.02 | 1.136 |
| final R indices [I > 4σ(I)] | R1 = 0.075, wR2 = 0.183 | R1 = 0.074, wR2 = 0.164 | R1 = 0.066, wR2 = 0.161 | R1 = 0.064, wR2 = 0.159 | R1 = 0.118, wR2 = 0.314 |
| R indices (all data) | R1 = 0.145, wR2 = 0.218 | R1 = 0.117, wR2 = 0.191 | R1 = 0.119, wR2 = 0.190 | R1 = 0.092, wR2 = 0.175 | R1 = 0.193, wR2 = 0.372 |
| largest diff peak/hole [e · Å ⁻³] | 0.551/–0.476 | 0.860/–0.423 | 0.538/–0.521 | 0.421/–0.364 | 1.325/–1.003 |

[R = H, R' = Me (3),¹⁵ Et (4), Ph (5), R = Me, R' = Me (6), Et (7), Ph (8)] (Scheme 2). Complexes 3–8 were isolated as orange-brown or reddish crystals in good yields (65–76%) upon slow reaction without stirring at room temperature and were characterized by IR spectrophotometry, ¹H and ¹³C NMR spectroscopy, mass spectrometry, C and H microanalysis, and X-ray diffraction analysis in the case of complexes 7 and 8 (see below). The air- and moisture-sensitive complexes 3–8 are scarcely soluble in hexane and soluble in aromatic solvents.

Scheme 2. Synthesis of Adducts 3–8



The ¹H NMR spectra for 3–5 reveal resonance signals for two types of C₅Me₅ ligands in a 2:1 ratio, consistent with C_s-symmetric structures in solution, signals for the μ₃-methylidyne group, and those corresponding to the alkyl and aryl ligands. On the other hand, for the complexes obtained from the μ₃-ethylidyne species 6 and 7, the NMR spectra exhibit, in addition to μ₃-ethylidyne and alkyl protons, only one broad signal for the C₅Me₅ groups coherent with a fluxional process in a benzene-*d*₆ solution at room temperature.

However, ¹H NMR spectroscopy reveals a C_s-symmetric structure at low temperature (*T* < 0 °C) according to Scheme 2 and the solid-state structure determined for compound 7 (see Figure 1). Moreover, the NMR spectrum of complex 8 already reveals at room temperature two signals for the C₅Me₅ ligands in a 2:1 ratio analogous to that found for complexes 3–5; it is in agreement with the solid-state structure (see Figure 2b), the Lewis acidity of AlPh₃, and the higher steric hindrance of the phenyl rings. Interestingly, the μ₃-C resonance signals of complexes 3–5 (δ 401.2–404.7) and 6–8 (δ 418.1–420.0) are shifted to lower field with respect to the μ₃-alkylidyne starting materials 1 [δ(μ₃-CH) 383.8] and 2 [δ(μ₃-CMe) 401.7], respectively. We have observed a similar behavior in the oxoheterometallobenzene derivatives [(CO)₃Mo-(μ₃-O)₃(η⁵-C₅Me₅)₃(μ₃-CR)] (R = H, δ 410.3; R = Me, δ 434.8).⁷ The parent ion was not observed in the EI-MS spectra, but related fragments such as [M – AIR'₃]⁺ (R = Me, Et, Ph) were detected for all of the synthesized complexes.

The solid-state structures of 7 and 8 determined by single-crystal X-ray diffraction are shown in Figures 1 and 2, while a selection of lengths and angles are summarized in Tables 2 and 3. The molecular structures of 7 and 8 reveal how the organometallic ligand 2 can coordinate to the incorporated aluminum center in a monodentate way. The aluminum atom exhibits a distorted tetrahedral geometry, comprising three ethyl or phenyl

groups and one oxygen atom from the oxo ligand **2** with the average angles spanning $102.7(2)$ – $109.0(3)^\circ$, in the same range as that observed for other triorganoaluminum oxo adduct complexes.¹⁶

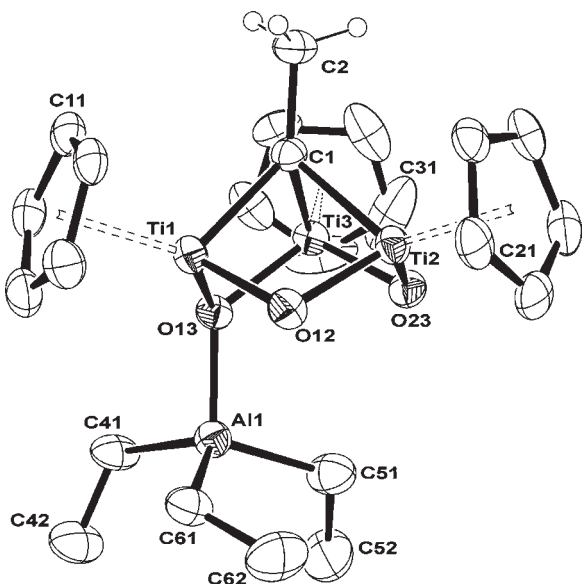


Figure 1. Molecular structure of **7** with thermal ellipsoids at the 50% probability level. Methyl groups of the pentamethylcyclopentadienyl ligands and hydrogen atoms except those of the ethylidene ligand have been omitted for clarity.

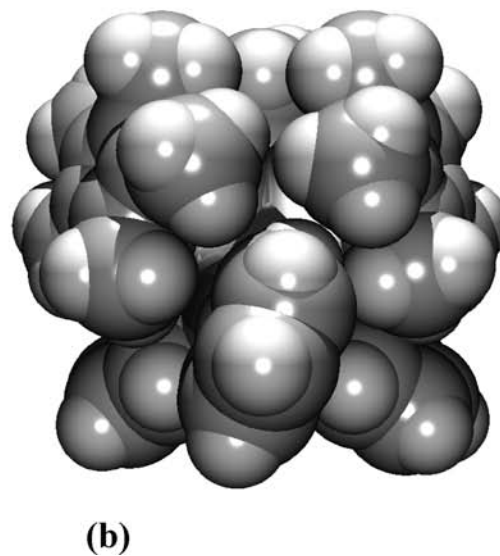
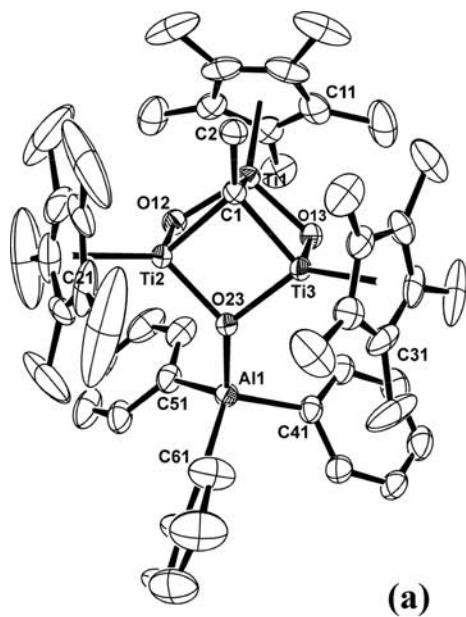


Figure 2. (a) Molecular structure of **8** with thermal ellipsoids at the 50% probability level. Hydrogen atoms have been omitted for clarity. (b) Space-filling model of **8**.

Table 2. Selected Bond Lengths (Å) and Angles (deg) for **7**

| | | | |
|------------------------|----------|----------------------------|----------|
| C1–C2 | 1.533(6) | Ti–C1–Ti | 85.0(2) |
| C1–Ti1 | 2.102(4) | Ti1–O13–Ti3 | 97.8(1) |
| C1–Ti2 | 2.166(4) | Ti–O–Ti2 | 101.7(1) |
| C1–Ti3 | 2.091(4) | O23–Ti2–O12 | 107.7(1) |
| Ti–O13 | 1.921(3) | O13–Ti–O _{bridge} | 100.6(2) |
| Ti–O _{bridge} | 1.838(2) | All–O13–Ti1 | 121.4(1) |
| All–C | 2.008(4) | All–O13–Ti3 | 123.6(1) |
| All–O13 | 1.909(3) | O13–All–C41 | 102.7(2) |
| Ti···Ti | 2.87(2) | O13–Al–C | 108.2(2) |

Table 3. Selected Bond Lengths (Å) and Angles (deg) for **8**

| | | | |
|------------------------|----------|----------------------------|----------|
| C1–C2 | 1.520(6) | Ti–C1–Ti | 85.0(2) |
| C1–Ti1 | 2.164(4) | Ti2–O23–Ti3 | 96.3(1) |
| C1–Ti2 | 2.095(4) | Ti–O–Ti1 | 102.1(2) |
| C1–Ti3 | 2.078(4) | O12–Ti1–O13 | 106.5(1) |
| Ti–O23 | 1.938(3) | O23–Ti–O _{bridge} | 100.5(9) |
| Ti–O _{bridge} | 1.827(7) | All–O23–Ti2 | 125.7(1) |
| All–C | 1.990(5) | All–O23–Ti3 | 126.3(1) |
| All–O23 | 1.878(3) | O23–All–C | 109.0(3) |
| Ti···Ti | 2.86(2) | | |

Although the aluminum substituents in **7** and **8** present an eclipsed conformation with respect to the bulky pentamethylcyclopentadienyl rings linked to the closest titanium atoms, to minimize steric repulsion, the C41–C42 and C51–C52 ethyl groups are pointing down with respect to the organometallic ligand **2** in complex **7**, while the existing free space below O12 allows the third ethyl group to show an angle of $25.4(2)^\circ$ with the plane formed by the three titanium atoms instead of the averaged $63.4(4)^\circ$ found for the other two.¹⁷ This difference avoids using the propeller-like term to describe the arrangement of the triethylaluminum fragment with respect to the organometallic ligand in complex **7**. On the other hand, the higher steric hindrance of the ligands joined to aluminum in **8** leads the C41–C46 and C51–C56 phenyl rings to be close to the bulky pentamethylcyclopentadienyl rings (see Figure 2b) and shows angles with respect to the Ti₃ plane of $35.2(2)^\circ$ and $36.8(2)^\circ$, respectively. On the other hand, the C61–C66 phenyl ring, which is pointing outside the oxo ligand but in the existing space between two pentamethylcyclopentadienyl groups, presents a value of $70.9(2)^\circ$ for the same angle.

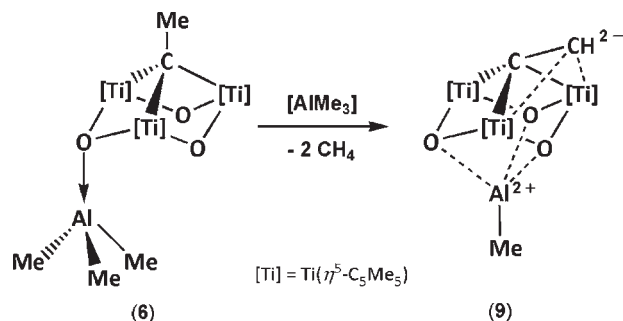
Examination of the data shows that the C–Al distances in both complexes range from 1.984(5) to 2.014(5) Å and are similar to those observed in other organoaluminum adducts that lie in the range 1.93–1.99 Å¹⁶ and to the dimeric [AlMe₃]¹⁸ (Al–Me terminal: 1.957 and 1.983 Å).

The Al–O bond lengths of 1.909(3) Å in **7** and 1.878(3) Å in **8** are similar to that found in the ether adduct of

[Al(CH₂Ph)₃(OEt₂)] [1.901(4) Å]¹⁹ but shorter than those found for the [Al(*o*-Tol)₃(OEt₂)] (1.980 Å),²⁰ [Al(Me)₃-THF] (1.969 Å),^{16a} [(AlMe₃)₂(*p*-dioxane)] [2.02(2) Å],²¹ [(AlMe₃)₄(15-crown-5)] [2.005(6) Å],²² and [(AlMe₃)₂-(dibenzo-18-crown-6)] [1.967(3) Å]²² adducts of trimethylaluminum.

Compounds **3–8** undergo methane, ethane, or benzene loss together with a μ_3 -alkylidyne starting material and other unidentified compounds when left at room temperature in solution for several days. In order to gain knowledge about these processes and avoid the presence of a free μ_3 -alkylidyne, we decided to add a stoichiometric excess (1:2 or 1:3) of trialkyl- or triarylaluminum derivatives to solutions of the μ_3 -alkylidyne species but, unfortunately, it was not possible to identify spectroscopically any of the expected adducts and intractable mixtures of the products were obtained. Only when the reaction of complex **6** with 1 equiv of [AlMe₃] was carried out in toluene at room temperature for 20 days were we able to isolate and characterize, by the usual methods, the new compound **9** shown in Scheme 3. Following workup, compound **9** was isolated as a black solid in 48% yield and characterized by IR and NMR spectroscopy, mass spectrometry, and microanalysis, as summarized in the Experimental Section.

Scheme 3. Synthesis of Complex 9



NMR spectra of compound **9** reveal the equivalence of two of the three η^5 -C₅Me₅ ligands, with two signals in a 2:1 ratio in the ¹H NMR spectrum (δ 1.81 and 2.13) and four in the ¹³C{¹H} NMR [δ 118.1 and 120.7 (C₅Me₅), 11.4 and 12.07 (C₅Me₅), consistent with a C_s symmetry. Also, the NMR spectra display a singlet at δ -0.50 with an integrated intensity of 3H in the ¹H NMR and a singlet at δ -17.9 in the ¹³C{¹H} NMR, assigned to the methyl group joined to the aluminum atom. Otherwise, the spectra contain a singlet at δ 9.42 in the ¹H NMR with an integrated intensity of 1H and a doublet at δ 235.5 ($J_{\text{CH}} =$

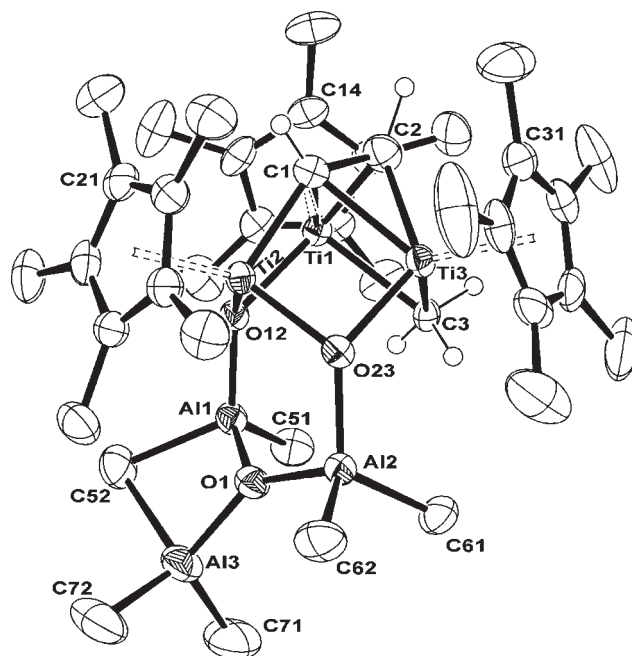


Figure 3. Molecular structure of **10** with thermal ellipsoids at the 50% probability level.

Table 4. Selected Bond Lengths (Å) and Angles (deg) for **10**

| | | | |
|-------------|----------|--------------------------|----------|
| C1–C2 | 1.402(6) | Ti3–O23 | 2.023(3) |
| C1–Ti1 | 2.242(4) | Al1–O1 | 1.810(3) |
| C1–Ti2 | 2.068(4) | Al2–O1 | 1.824(3) |
| C1–Ti3 | 2.245(4) | Al3–O1 | 1.807(3) |
| C2–Ti3 | 2.086(4) | Al1–O12 | 1.785(3) |
| C2–Ti1 | 2.087(5) | Al2–O23 | 1.840(3) |
| C3–Ti3 | 2.314(4) | Al–C _{terminal} | 1.979(9) |
| C3–Ti1 | 2.315(4) | Al1–C52 | 2.090(5) |
| Ti1–O12 | 2.055(3) | Al3–C52 | 2.297(6) |
| Ti2–O12 | 1.979(3) | Ti···Ti | 2.859(7) |
| Ti2–O23 | 1.952(2) | | |
| <hr/> | | | |
| Ti2–C1–C2 | 137.8(3) | Ti2–O12–Al1 | 122.3(2) |
| Ti1–C3–Ti3 | 76.3(1) | Ti1–O12–Al1 | 128.1(2) |
| Ti1–O12–Ti2 | 90.6(1) | Al1–O1–Al2 | 126.0(2) |
| Ti2–O23–Ti3 | 91.6(1) | Al1–O1–Al3 | 94.9(2) |
| Ti2–O23–Al2 | 126.0(2) | Al2–O1–Al3 | 137.4(2) |
| Ti3–O23–Al2 | 131.7(2) | Al1–C52–Al3 | 74.6(2) |

182 Hz) in the ¹³C NMR, attributed to the fragment –CH^{2–}. The apical carbon, μ_3 -C, shows a singlet at δ 329.4, shifted to higher field with respect to **2** [$\delta(\mu_3\text{-CMe}) = 401.7$] in a way similar to that found in other dehydration processes of **2**.^{9b,c} These data are coherent with the structure depicted in Scheme 3, where we propose the coordination of the three oxygen atoms of the Ti₃O₃ ring to the [AlMe] fragment and the double dehydration of the μ_3 -CMe apical fragment, in a way similar to that reported by us for the compound [Mg(μ_4 -O)(μ_3 -O)₂{Ti₃(η^5 -C₅Me₅)₃-(μ_3 -CCH)}₂].^{9c}

To carefully study the formation of **9**, the reaction of the starting material **2** and 2 equiv of [AlMe₃] in C₆D₆ was monitored by ¹H NMR spectroscopy. Initially, the reaction progressed with the formation of adduct **6**, and after several days at room temperature, complex **9** and methane elimination were observed. No other different compound was detected in the NMR tube test.

In one of the many attempts carried out to isolate **9** in good yield, a pentane solution of **6** with an excess of trimethylaluminum was heated at 100 °C for several days.

(15) González-del Moral, O.; Hernán-Gómez, A.; Martín, A.; Mena, M.; Santamaría, C. *Dalton Trans.* **2008**, 44–46.

(16) De Mel, V. S. J.; Oliver, J. P. *Organometallics* **1989**, *8*, 827–830 and references cited therein. (b) Holloway, C. E.; Melnik, M. *J. Organomet. Chem.* **1997**, *543*, 1–37 and references cited therein.

(17) PARST: (a) Nardelli, M. *Comput. Chem.* **1983**, *7*, 95–97. (b) Nardelli, M. *J. Appl. Crystallogr.* **1995**, *28*, 659.

(18) Vranka, R. G.; Amma, E. L. *J. Am. Chem. Soc.* **1967**, *89*, 3121–3126.

(19) Maqsidur Rahman, A. F. M.; Siddiqui, K. F.; Oliver, J. P. *J. Organomet. Chem.* **1987**, *319*, 161–166.

(20) Barber, M.; Liptak, D.; Oliver, J. P. *Organometallics* **1982**, *1*, 1307–1311.

(21) Atwood, J. L.; Stucky, G. D. *J. Am. Chem. Soc.* **1967**, *89*, 5362–5366.

(22) Atwood, J. L.; Hrnčir, D. C.; Shakir, R.; Dalton, M. S.; Priester, R. D.; Rogers, R. D. *Organometallics* **1982**, *1*, 1021–1025.

A slow cooling of the reaction mixture at room temperature allowed us to obtain a few single crystals of the complex **10** shown in Figure 3. A selection of bond lengths and angles for **10** appears in Table 4. Unfortunately, all new attempts to isolate **10** in those conditions were unsuccessful, and no further characterization was possible.

The main motif of the molecular structure of complex **10** can be described as a $[\text{Ti}_3\text{O}_2\text{C}]$ core (see Figure 3), with each titanium atom linked to a pentamethylcyclopentadienyl ligand, which supports a $\mu_3\text{-}\eta^2\text{-HCCH}$ fragment on one side of the Ti_3 plane, while it is coordinated to a $\{(\text{AlMe}_2)_2(\text{AlMe})(\mu\text{-CH}_3)(\mu_3\text{-O})\}$ unit through two oxygen atoms of the core on the opposite side.

As can be seen in Figure 3, the solid-state structure of complex **10** shows that the starting μ_3 -alkylidyne group of the organometallic ligand **2** has suffered dehydrogenation to give the carbanion $\mu_3\text{-CCH}_2^-$ fragment;^{9b,c} then a 1,2-hydrogen migration process leads to the formation of a $\mu_3\text{-}\eta^2\text{-HCCH}^-$ ligand linked to the three titanium atoms. The structural disposition of this moiety with respect to the titanium atoms is similar to those observed for some trinuclear clusters with alkyne ligands²³ and to that reported for the incorporation of alkaline-earth derivatives to complex **2**.^{9c}

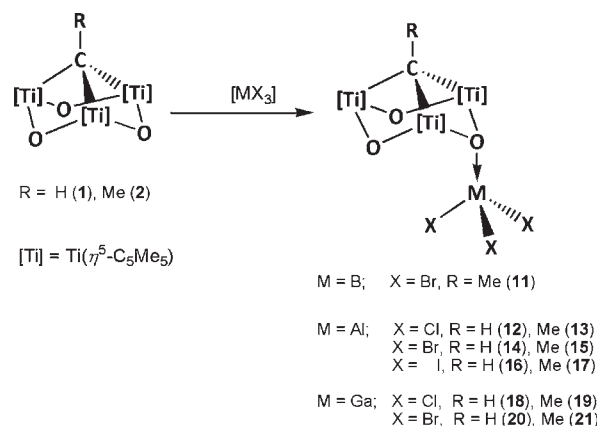
On the other hand, one of the bridging oxygen atoms of the Ti_3O_3 ring has been replaced by a methyl group process, and it is now bonded to three aluminum atoms. Bond distances for the $\text{Ti-CH}_3\text{-Ti}$ fragment are only slightly longer than those reported for the complex $\{[\text{bis}(\text{amidinate})]\text{Ti}_2\text{Cp}_2(\mu\text{-CH}_3)(\mu\text{-H})\}$,²⁴ while the parameters found for the $\{(\text{AlMe}_2)_2(\text{AlMe})(\mu\text{-CH}_3)(\mu_3\text{-O})\}$ unit are in the range found for other compounds containing three alkylaluminum fragments bonded to one oxygen atom.²⁵

Some details about the reactions carried out between the starting materials **1** or **2** and different haloalkylaluminum derivatives can be found in the Supporting Information.

Coordination of $\{[\text{Ti}(\eta^5\text{-C}_5\text{Me}_5)(\mu\text{-O})]_3(\mu_3\text{-CR})\}$ [R** = **H** (**1**), **Me** (**2**)] to MX_3 (**M** = **B**, **X** = **Br**; **M** = **Al**, **X** = **Cl**, **Br**, **I**; **M** = **Ga**, **X** = **Cl**, **Br**).** The reaction of 1 equiv of the corresponding trihalide derivative in toluene solutions with the μ_3 -alkylidyne species **1** or **2** produced in all cases the formation of a series of complexes with the general formula $[\{X_3M\}(\mu_3\text{-O})(\mu\text{-O})_2\{\text{Ti}(\eta^5\text{-C}_5\text{Me}_5)\}_3(\mu_3\text{-CR})]$ on the basis of analytical and spectroscopic data; see the Experimental Section. The air- and moisture-sensitive complexes **11–21** were obtained in moderate yields (32–62%) as brown or reddish solids. Compounds **11**, **12**, **14**, **16**, **18**, and **20** are scarcely soluble in saturated hydrocarbons and aromatic solvents, while **13**, **15**, **17**, **19**, and **21** are soluble in chloroform.

Complexes **11–21** were characterized by spectroscopic and analytical techniques, as well as by single-crystal X-ray diffraction analysis in the case of **13**. In a fashion

Scheme 4. Synthesis of Adducts **11–21**



similar to that found for the previously synthesized complexes, the ^1H and ^{13}C NMR spectra in benzene- d_6 show resonance signals for two types of $\eta^5\text{-C}_5\text{Me}_5$ ligands, consistent with the structure outlined in Scheme 4. Once again, the apical carbon, $\mu_3\text{-C}$, shows a singlet in the range δ 406.2–410.8 for **12**, **14**, **16**, **18**, and **20** and δ 425.5–427.1 for **13**, **15**, **17**, **19**, and **21**, slightly shifted to lower field with respect to **1** [$\delta(\mu_3\text{-CH}) = 383.8$] and **2** [$\delta(\mu_3\text{-CMe}) = 401.7$], respectively. It is interesting to note that while complexes **12–21** exhibit the same resonance signal scheme for the pentamethylcyclopentadienyl rings in the ^1H NMR spectra, compound **11** shows an inverted order for the resonance intensities, which are slightly shifted (δ 2.00 and 2.18) to lower field with respect to those of the analogous compounds **13**, **15**, **17**, **19**, and **21** (δ 1.95–2.08). Additionally, in the ^{13}C NMR spectrum, the signal at δ 499.4, attributed to the $\mu_3\text{-CMe}$ apical carbon, is shifted significantly downfield. These shifts could be the result of the higher electronegativity and smaller size of the boron atom as head of the group with respect to the other group 13 elements.

Single crystals of **13** suitable for X-ray diffraction analysis were grown from hexane at room temperature. The molecular structure is shown in Figure 4, while the most relevant parameters are summarized in Table 5 and demonstrate how complex **2** is coordinated to the AlCl_3 unit through O12 in a monodentate way, providing a tetrahedral environment for the aluminum atom. The Al1–O12 distance of 1.797(5) Å is slightly shorter than those found for complexes **7** and **8** but similar to those reported for other complexes where the AlCl_3 moiety is linked to a bridging or terminal oxygen atom.²⁶ The shortest Ti–C1 bond distances are found for the metal atoms joined to the coordinated oxygen atom O12; also the Ti–O12 distances are longer, and the Ti1–O12–Ti2 angle is $\approx 6^\circ$ narrower.

Finally, when a solution of **11** in toluene was allowed to stir for 2 days at room temperature, compound **22** could be obtained as orange crystals in a 35% yield after slow cooling to -35°C . Surprisingly, and in contrast with the rest of the compounds here reported, the NMR spectra of **22** revealed the nonequivalence of the three $\eta^5\text{-C}_5\text{Me}_5$

(23) (a) Nishioka, T.; Isobe, K.; Kinoshita, I.; Ozawa, Y.; Vazquez de Miguel, A.; Nakai, T.; Miyajima, S. *Organometallics* **1998**, *17*, 1637–1639. (b) Sappa, E.; Tiripicchio, A.; Braunstein, P. *Chem. Rev.* **1983**, *83*, 203–239.

(24) Hagadorn, J. R.; McNevin, M. J. *Organometallics* **2003**, *22*, 609–611.

(25) (a) Atwood, J. L.; Hrcncir, D. C.; Priester, R. D.; Rogers, R. D. *Organometallics* **1983**, *2*, 985–989. (b) Wei, P.; Stephan, D. W. *Organometallics* **2003**, *22*, 1992–1994.

(26) (a) Engelhardt, L. M.; Junk, P. C.; Raston, C. L.; Skelton, B. W.; White, A. H. *J. Chem. Soc., Dalton Trans.* **1996**, 3297–3301. (b) Calderazzo, F.; Englert, U.; Pampaloni, G.; Santi, R.; Sommazzi, A.; Zinna, M. *Dalton Trans.* **2005**, 914–922.

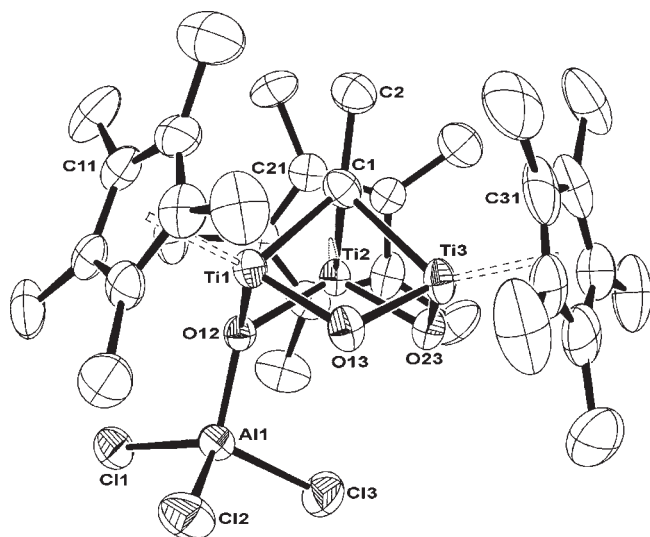


Figure 4. Molecular structure of **13** with thermal ellipsoids at the 50% probability level. Hydrogen atoms have been omitted for clarity.

Table 5. Selected Bond Lengths (Å) and Angles (deg) for **13**

| | | | |
|-------------|-----------|------------------------|----------|
| C1–C2 | 1.501(10) | Ti2–O12 | 1.983(4) |
| C1–Ti1 | 2.108(7) | Ti–O _{bridge} | 1.842(9) |
| C1–Ti2 | 2.138(7) | Al1–Cl | 2.145(8) |
| C1–Ti3 | 2.180(7) | Al1–O12 | 1.797(5) |
| Ti1–O12 | 1.979(4) | Ti···Ti | 2.89(4) |
| | | | |
| Ti1–C1–Ti2 | 87.6(3) | O23–Ti3–O13 | 107.0(2) |
| Ti–C1–Ti3 | 83.4(3) | Al1–O12–Ti1 | 128.5(2) |
| Ti1–O12–Ti2 | 95.7(2) | Al1–O12–Ti2 | 122.2(2) |
| Ti–O–Ti3 | 101.9(2) | O12–Al1–Cl | 109(1) |
| O13–Ti1–O12 | 100.6(2) | | |

ligands, with three signals in a 1:1:1 ratio in the ^1H NMR spectrum (δ 2.07, 2.10, and 2.21) and six in the ^{13}C NMR [δ 124.8, 126.5, and 133.6 (C_5Me_5), 11.6, 12.8, and 14.1 (C_5Me_5)], consistent with a lower symmetry in the molecule. Also noticeable was the upfield shift observed in the ^{13}C NMR spectrum for the methyl group of the μ_3 -alkylidyne moiety from δ 44.5 in **11** to δ 20.9 in **22**. These data, together with the MS spectrum, made us suspect that the molecular structure of this compound could not be like those found for the rest of the adducts, so a single-crystal X-ray diffraction study was performed.

As shown in Figure 5, the molecular structure of **22** reveals how the Ti_3O_3 ring, the core unit for all of the adducts, has been broken and now the boron atom appears as a link between one of the old central $[\text{Ti}(\eta^5\text{-C}_5\text{Me}_5)(\mu\text{-O})]$ units and the rest of the molecule, arising as a boronate fragment. This disposition forces the μ_3 -alkylidyne fragment to be linked to two titanium atoms and the bridging boron. On the other hand, the bromine atoms of the existing BBr_3 in **11** now fill the vacant valences in the Ti1 and Ti3 atoms. Curiously, a few structures in the CSD²⁷ contain a transition metal–oxygen–boron–carbon connectivity, but none of them with a μ_3 -alkylidyne moiety.

All of the titanium atoms present the typical three-legged piano-stool environment with the Ti–C1 bond distance slightly shorter than those found for other

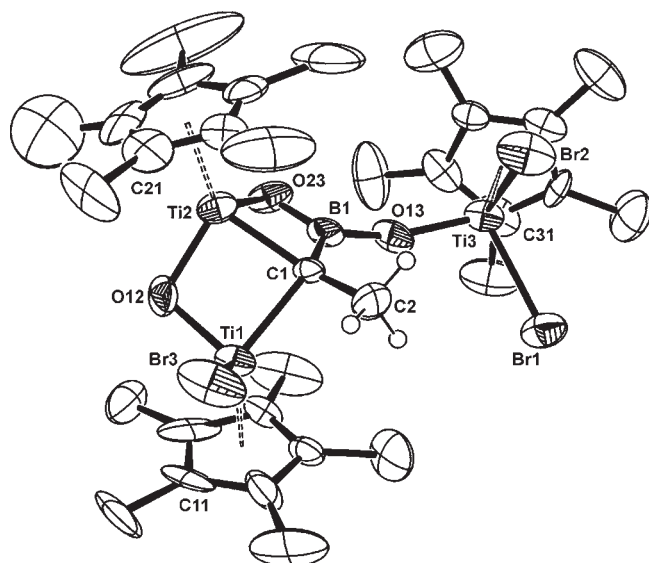


Figure 5. Molecular structure of **22** with thermal ellipsoids at the 50% probability level. Hydrogen atoms of the pentamethylcyclopentadienyl groups have been omitted for clarity.

Table 6. Selected Bond Lengths (Å) and Angles (deg) for **22**

| | | | |
|-------------|-----------|-------------|-----------|
| Ti1–C1 | 2.086(12) | B1–C1 | 1.59(2) |
| Ti2–C1 | 2.028(13) | B1–O23 | 1.35(2) |
| Ti1–O12 | 1.801(11) | B1–O13 | 1.36(2) |
| Ti2–O12 | 1.862(10) | Ti3–O13 | 1.803(11) |
| Ti1–Br3 | 2.469(3) | Ti3–Br1 | 2.423(3) |
| Ti2–O23 | 1.885(10) | Ti3–Br2 | 2.406(3) |
| | | | |
| Ti1–C1–Ti2 | 86.4(5) | C1–B1–O13 | 119.1(13) |
| Ti1–C1–B1 | 125.7(9) | C1–B1–O23 | 115.4(13) |
| Ti1–O12–Ti2 | 100.6(5) | O13–B1–O23 | 125.5(12) |
| Ti2–O23–B1 | 87.7(8) | B1–O13–Ti3 | 161.2(10) |
| C2–C1–B1 | 121.5(12) | O13–Ti3–Br1 | 103.4(3) |
| C2–C1–Ti1 | 95.9(8) | O13–Ti3–Br2 | 99.9(3) |
| C2–C1–Ti2 | 152.8(10) | | |

adducts here described and Ti–O bond lengths similar to those reported for the boroxide derivatives $[\text{Ti}\{\text{OB}(\text{mes})_2\}_3(\text{CH}_2\text{Ph})]$ (av 1.794 Å)²⁸ and $[\text{TiCp}_2\{\text{OB}(\text{mes})_2\}\text{-Cl}]$ [1.888(2) Å].²⁹ Further, the average B–O distance of 1.36(1) Å is also similar to those of the mentioned boroxide complexes but shorter than that reported for the dinuclear complex $[\{\text{TiCl}_2(\mu\text{-}\{\text{OB}(\text{NHMe}_2)\text{-}\eta^5\text{-C}_5\text{H}_4\})\}_2\text{-}\mu\text{-O}]$ [1.486(3) Å], where the boron and titanium atoms are also linked by a bridging oxygen atom (Table 6).³⁰

Conclusion

A family of structurally novel adducts containing the pre-organized ligands $[\{\text{Ti}(\eta^5\text{-C}_5\text{Me}_5)\}_3(\mu_3\text{-O})(\mu_3\text{-CR})]$ (R = H, Me) and group 13 derivatives have been obtained. The new complexes locate the incorporated inorganic fragment on the periphery of the organometallic oxides and reveal how these trinuclear oxotitanium systems are also capable of acting as monodentate ligands. The careful choice of the reaction conditions allowed the synthesis of pure compounds; however,

(28) Cole, S. C.; Coles, M. P.; Hitchcock, P. B. *Dalton Trans.* **2004**, 3428–3430.

(29) Cole, S. C.; Coles, M. P.; Hitchcock, P. B. *Organometallics* **2005**, *24*, 3279–3289.

(30) Braunschweig, H.; Breiting, F. M.; Burschka, C.; Seeler, F. *J. Organomet. Chem.* **2006**, *691*, 702–710.

(27) Allen, F. H. *Acta Crystallogr.* **2002**, *B58*, 380–388.

the group 13 fragments show a remarkable tendency to produce building bridges, although being coordinated. On the other hand, some of the incorporated fragments are able to develop rupture processes in the $[\text{Ti}_3\text{O}_3]$ ring.

Acknowledgment. Financial support for this work was provided by the Ministerio de Ciencia e Innovación (CTQ2008-00061/BQU) and Factoría de Cristalización

(CONSOLIDER-INGENIO 2010). A.H.-G. thanks the MEC for a doctoral fellowship.

Supporting Information Available: X-ray crystallographic files in CIF format for complexes **7**, **8**, **10**, **13**, and **22**, overview of the reactions carried out between **1** or **2** with haloalkylaluminum derivatives, and X-ray details about the crystal structure of complex S5. This material is available free of charge via the Internet at <http://pubs.acs.org>.